HHS Public Access

Author manuscript

Neurobiol Aging. Author manuscript; available in PMC 2020 November 02.

Published in final edited form as:

Neurobiol Aging. 2020 September ; 93: 25–34. doi:10.1016/j.neurobiolaging.2020.04.013.

Older, non-demented apolipoprotein ε_4 carrier males show hyperactivation and structural differences in odor memory regions: a blood-oxygen-level-dependent and structural magnetic resonance imaging study

Eleni A. Kapoulea[a], **Claire Murphy**[a,b,c,*]

[a]Department of Psychology, San Diego State University, San Diego, CA, USA

[b]San Diego Joint Doctoral Program in Clinical Psychology, San Diego State University/University of California, San Diego, San Diego, CA, USA

[c]Department of Psychiatry, University of California, San Diego, San Diego, CA, USA

Abstract

The current study sought to examine the interaction of sex and Apolipoprotein ε_4 status on olfactory recognition memory within non-demented, older individuals. We separated 39 participants into groups based on ε_4 status and sex. Each participant completed an olfactory memory recognition task during 2 functional magnetic resonance imaging scans and 1 structural scan. The ε_4 carriers had greater functional recruitment of memory regions during false positives relative to ε_4 non-carriers. During hits, the male ε_4 carriers showed greater functional recruitment compared to female ε_4 carriers. The ε_4 carriers had larger bilateral putamen volumes relative to ε_4 non-carriers. Neuroimaging data were significantly associated with Dementia Rating Scale scores solely in males. Results suggest differential olfactory memory processing in relation to sex and ε_4 status. Male ε_4 carriers in particular, demonstrated hyperactivation during recognition memory, which we suspect reflects neuronal compensation to maintain functional performance. Future studies should consider examining underlying mechanisms that contribute to these sex differences within ε_4 carriers.

Keywords

Alzheimer's disease; Apolipoprotein ε_4; Olfactory memory; Neuroimaging; Sex

*Corresponding author at: San Diego Joint Doctoral Program in Clinical Psychology, San Diego State University/University of California, San Diego, 6363 Alvarado Ct. San Diego, CA 92120-4913, USA. Tel.: 619 594 4559; fax: 619 594 6780. cmurphy@sdsu.edu (C. Murphy).

CRediT authorship contribution statement

Eleni A. Kapoulea: Conceptualization, Methodology, Formal analysis, Writing - original draft, Visualization. **Claire Murphy:** Conceptualization, Methodology, Resources, Writing - review & editing, Supervision, Project administration, Funding acquisition.

Disclosure statement

The authors have no actual or potential conflicts of interest.

Appendix A. Supplementary data

Supplementary data to this article can be found online at https://doi.org/10.1016/j.neurobiolaging.2020.04.013.

1. Introduction

The presence of the Apolipoprotein (ApoE) ε_4 allele is the most well-established genetic risk factor for Alzheimer's disease (AD), a devastating neurodegenerative disease with no cure (Alzheimer's Association, 2018; Bu, 2009). In humans, the ApoE gene exists as 3 different polymorphic alleles (ε_2, ε_3, ε_4; Bu, 2009; Farrer et al., 1997; Lind et al., 2006; Yu et al., 2013). Under normal physiological conditions, ApoE supports cholesterol and lipid transport and performs membrane repair processes to protect neuronal integrity (Mahley and Huang, 2012). The ε_4 variant generally exhibits poorer cholesterol transport and amyloid-β (Aβ) plaque clearance, as well as increased neurofibrillary tangle formation relative to the ε_3 allele (Mahley and Rall, 2000). The accumulation of neurofibrillary Aβ plaques and tau tangles is a pathological marker in AD and associated with cognitive decline (Blennow et al., 2006; Braak and Braak, 1991, 1996; Hedden et al., 2013). These accumulations are often reported in medial temporal lobe (MTL) regions (e.g., entorhinal cortex [ERC], hippocampus), which are areas associated with odor recognition memory (Cerf-Ducastel and Murphy, 2009).

Sex differences in odor identification (odor ID) and AD development have been noted in previous literature. Older women tend to outperform older men in odor ID tasks (Murphy et al., 2002; Wehling et al., 2016). Males' ability to identify odors may deteriorate earlier (approximately 20 years) in the lifespan relative to females (Ship et al., 1996). The ApoE ε_4 allele tends to have a more pronounced effect on late-onset AD development in women compared to men, although some attribute this to women's longer lifespan (Altmann et al., 2014; Bartrés-Faz et al., 2002; Holland et al., 2013; Hyman et al., 1996; Payami et al., 1996; Poirier et al., 1993; Ungar et al., 2014). Women homozygous for ε_4 have a greater risk than heterozygous women, but male homozygous and heterozygous for the ε_4 allele do not differ significantly (Payami et al., 1996). Despite the apparent sex differences in AD progression, it is relatively overlooked in the existing literature (Ungar et al., 2014).

Participants with and at-risk for AD have demonstrated poor recognition memory overall, with olfactory recognition memory being the most compromised (Moberg et al., 1987). Individuals at-risk for AD but who have not yet developed clinical dementia demonstrate deficits in olfactory functioning, particularly in olfactory memory, recall, and recognition (Albers et al., 2015; Murphy, 2019; Murphy et al., 1999; Nordin and Murphy, 1996, 2006; Olofsson et al., 2010). Participants with selective odor memory deficits are significantly more likely to possess the ε_4 allele (Albers et al., 2016). Odor recognition memory and odor ID are most impaired in ε4 carriers relative to other memory tasks (e.g., picture ID, facial recognition memory; Calhoun-Haney and Murphy, 2005; Gilbert and Murphy, 2004).

The brain regions that are impacted by AD overlap with brain regions that are critical for olfaction. Early projections of the olfactory system involve MTL brain regions that are involved in the encoding and retrieval of episodic memories, such as the ERC and hippocampus (Cerf-Ducastel and Murphy, 2009; Haase et al., 2013). Those with odor memory deficits demonstrate significantly reduced ERC thickness relative to those without deficits (Albers et al., 2016). Atrophy and plaque and tangle accumulation in the MTL are early pathological changes in AD progression (Albers et al., 2015; Attems et al., 2005, 2014;

Braak and Braak, 1991, 1996, 1997; Esiri and Wilcock, 1984; Frisoni et al., 2010; Hyman, 1997; Murphy et al., 2003; Price et al., 1991; Stoub et al., 2006; Visser et al., 2002).

Although there are studies exploring neuroimaging data within ε_4 carriers and ε_4 non-carriers during episodic memory tasks and resting-state functional magnetic resonance imaging (fMRI) (Chen et al., 2015, 2016; Dowell et al., 2016; Filippini et al., 2009; Mondadori et al., 2007; Ungar et al., 2014), information is absent on the interaction of sex and ApoE ε_4 status on functional and structural neuroimaging during olfactory recognition memory processing.

In order to fill this gap in the current literature, we examined differential olfactory recognition memory processing within a sample of non-demented, older ApoE ε_4 carriers and ε_4 non-carriers using structural neuroimaging and blood-oxygen-level-dependent fMRI. We further examined how sex modifies olfactory recognition memory processing within this population.

1.1. Hypotheses

Our first hypothesis is that ε_4 carriers will demonstrate significantly less volume and thickness within brain regions associated with olfactory memory, such as the ERC and hippocampus, after adjusting for age and ICV. A second hypothesis is that while all ε_4 carriers will demonstrate significantly greater functional activation in brain regions associated with odor memory during FPs and significantly less activation during hits, this activation pattern will be most pronounced in male ε_4 carriers. Our third hypothesis is that neuroimaging data will be associated with Dementia Rating Scale (DRS) scores within all groups.

2. Materials and methods

The current study sample was taken from an archival dataset. The Institutional Review Boards both at San Diego State University and the University of California, San Diego had approved the research. The only study published to date on this dataset was Haase et al. (2013) which reported behavioral and functional connectivity analyses.

2.1. Participants

Participants (N = 39) ranged in age from 64 to 88 and were divided into one of the 4 groups based on ε_4 status and sex: male ε_4 carriers (n = 9), female ε_4 carriers (n = 9), male ε_4 non-carriers (n = 10), and female ε_4 non-carriers (n = 11). ApoE ε_4 status was determined through genomic testing. We performed a 2 (ε_4 status: carrier, non-carrier) × 2 (sex: male, female) multivariate analysis of variance on demographic variables, which included age, education in years, odor threshold (Murphy et al., 1990), odor ID (San Diego Odor Identification Test; Murphy et al., 2002), or DRS scores, a global measure of cognitive function (Mattis, 1998). There were no significant differences between groups in demographics based on E4 status, sex, or the E4 × sex interaction ($p > 0.05$; Table 1).

2.2. Neuroimaging procedure

Prior to scanning, participants were presented with 16 familiar odors, in random order, corresponding to the list A of the California Odor Learning Test (Murphy et al., 1997). During the scan, participants were presented with labels of odors and their task was to indicate if the label was an odor that was presented to them prior to the scan (target) or if it was not (foil) using a button box (Cerf-Ducastel and Murphy, 2009, 2006; Haase et al., 2013). Each participant completed 2 functional runs (6 minutes each) and a structural run. Target periods consisted of 7 targets and 2 foils. Foil periods consisted of 7 foils and 2 targets. This paradigm was adapted from Stark and Squire (2000a, 2000b). Participants discriminated between odors using a button box, pressing 1 if they recognized the odor as having been presented before the scan and 2 if not. For the purposes of our current study, we focused on hit (correctly identifying a target as a target) and false positive (FP; incorrectly identifying a foil as a target) responses.

2.3. Imaging acquisition

Functional images were collected first using a standard gradient echo EPI pulse sequence to acquire T2-weighted functional images (30 axial slices, field of view = 25 cm, resolution 4 × 4 × 4 mm^3, repetition time = 4 seconds, echo time = 30 ms, flip angle = 90°). Parameters used to acquire structural images were as follows: T1-weighted whole-brain fast spoiled gradient echo magnetic resonance imaging sequence, field of view = 25 cm, resolution = 1 × 1 × 1 mm^3, repetition time = 16 seconds, echo time = 4.4 m, flip angle = 18°.

2.3.1. Structural neuroimaging data—T1-weighted structural scans were processed using standard FreeSurfer automated processing procedures within the FreeSurfer image analysis suite, version 5.2.0 (http://surfer.nmr.mgh.harvard.edu; Dale and Sereno, 1993; Fischl and Dale, 2000; Fischl et al., 2001; Fischl et al., 2004a; Fischl et al., 1999a; Dale et al., 1999; Fischl et al., 1999, 2002, 2004; Han et al., 2006; Jovicich et al., 2006; Kuperberg et al., 2003; Reuter et al., 2010, 2012; Reuter and Fischl, 2011; Rosas et al., 2002; Salat et al., 2004; Ségonne et al., 2004, 2007; Sled et al., 1998). Cortical thickness and volumetric estimates of regions of interest were extracted from automatic surface parcellation labels using the Desikan/Killiany Atlas (Desikan et al., 2006).

2.3.2. Functional neuroimaging data—Imaging data were processed using FMRIB Software Library (Analysis Group, FMRIB, Oxford, UK) and Analysis of Functional NeuroImage (open source software), using 3dDeconvolve, on each participant's concatenated runs based on the specified contrast (e.g., activation during hits and FPs; Cox, 1996; Cox and Hyde, 1997; Gold et al., 1998; Smith et al., 2004; Zald and Pardo, 2000). The output from 3dDeconvolve contains fit coefficients (i.e., beta weights) for each voxel, indicating the amplitude of the signal model for each contrast, and corresponding *t*-statistics.

2.4. Statistical analyses

2.4.1. Task performance—We performed a 2 (sex: male, female) × 2 (ε_4 status: ε_4 non-carrier, ε_4 carrier) multivariate analysis of covariance (MANCOVA) on the hit rate sand FP rate for the 2 independent runs and their average performance (Table 2). The MANCOVA controlled for age.

2.4.2. Structural neuroimaging data—We performed a 2 (sex: male, female) × 2 (ε_4 status: ε_4 non-carrier, ε_4 carrier) MANCOVA on left/right hippocampal volumetric and left/right ERC thickness measurements (Table 3). The MANCOVA controlled for age and intracranial volume (ICV).

2.4.3. Functional neuroimaging data—We performed a set of independent voxel-wise samples *t*-tests in whole-brain functional activations between groups during hits and FPs. Each analysis controlled for age and ICV. In an attempt to control for type I error in all group analyses, we thresholded the individual voxels at $p \leq 0.015$ and group statistical maps were corrected for multiple comparisons at the cluster level using the Analysis of Functional NeuroImage program ClustSim to protect a whole-brain probability of FPs at an overall alpha of 0.05 (Zald and Pardo, 2000). For an overall alpha level of 0.05, a cluster threshold of 21 contiguous voxels was applied.

2.4.4. Partial correlations—We performed a series of partial correlational analyses to examine associations between DRS scores and neuroimaging data. For correlations examining the association between structural measurements and DRS scores, partial correlations controlled for age and ICV. These correlations used a corrected alpha level of 0.004, which was calculated by dividing the original alpha level of 0.05 by the product of the number of groups (4) and the number of predictors (3).

If we examined the relationship between beta coefficients and DRS scores, each partial correlation controlled for age, ICV, and volume of the structure we were evaluating. These partial correlations used a corrected alpha level of 0.003, which was calculated by dividing the original alpha level of 0.05 by 16, the product of the number of groups (4) and the number of predictors (4).

3. Results

3.1. Task performance

Females demonstrated a significantly higher hit rate in run 1 when compared to males (M_F = 0.605 vs. M_M = 0.500, p = 0.04). The ε_4 carrier group also demonstrated significantly higher hit rates in run 1 when compared to ε_4 non-carriers (M_+ = 0.616 vs. M_- = 0.501; p = 0.01).

We found no significant main effects of sex or ε_4 status on run 2 hit rates or FP rates. There were also no significant interaction effects of the ε4 × sex interaction on hit or FP rates (p > 0.05). The results of this multivariate analysis of variance are summarized in Table 2.

3.2. Structural neuroimaging data

Table 3 summarizes group differences in hippocampal volume and ERC thickness. Females demonstrated significantly larger left hippocampal volumes (M_F = 3156.80 vs. M_M = 2823.79; p = 0.022) and right hippocampal volumes relative to males (M_F = 3360.65 vs. M_M = 2957.21; p = 0.006). For the right ERC thickness dependent variable, the ε4 status × sex interaction effect was statistically significant (p = 0.020). However, when simple effects tests were conducted to probe the interaction, we found no statistically significant (p > 0.0125) simple effects of ε_4 status at any level of sex or of sex at any level of ε_4 status.

3.3. Functional neuroimaging data

3.3.1. Hits—When functional activations of ApoE ε_4 carriers were subtracted from functional activations of ApoE ε4 non-carriers during hits, no significant differences were found between groups.

When functional activations during hits of ε_4 carrier females were subtracted from functional activations of ε_4 carrier males, males demonstrated significantly greater activation than females in the ApoE ε_4 carrier group in the anterior cingulate cortex (ACC), Brodmann's area (BA) 10, cuneus, precuneus, middle temporal gyrus, caudate, and putamen (Fig. 1A; Supplementary Materials A).

When functional activation of ApoE ε_4 non-carrier males was subtracted from ApoE ε_4 non-carrier females, there were no statistically significant differences between groups.

3.3.2. False positives—When functional activations of ApoE ε4 non-carriers were subtracted from functional activations of ApoE ε_4 carriers during FPs, ε_4 carriers demonstrated significantly greater activation than ε_4 carriers in the middle temporal gyrus, cuneus, precuneus, and right posterior cingulate cortex (PCC; Fig. 1B; Supplementary Materials B).

When functional activations of ApoE ε_4 carrier females were subtracted from ApoE ε_4 carrier males, females demonstrated significantly greater functional activation in areas associated with visual processing, such as the inferior and middle occipital gyrus (Fig. 1C; Supplementary Materials C).

We found no significant differences between males and females in the ε_4 non-carrier group during FPs.

3.4. Partial correlational analyses: neuroimaging data

We found no significant ($p > 0.004$) associations between beta coefficients and DRS scores in any of the 4 groups. Male ε_4 non-carriers demonstrated a significant, negative association between right hippocampal volume and DRS scores ($r = -0.888$, $p = 0.003$; Fig. 2B).

3.5. Post hoc analyses

3.5.1. Structural neuroimaging data—We performed exploratory analyses in order to further observe differences between groups. A 2 (sex: male, female) × 2 (ε_4 status: non-carrier, carrier) between-subjects MANCOVA was performed on 8 dependent variables: left/right caudate volume, left/right putamen volume, left/right isthmus cingulate thickness, and left/right parahippocampal thickness (Table 4). The MANCOVA controlled for age and ICV.

The caudate and putamen make up the dorsal striatum, which is affected by amyloid and tau pathology (Alexander et al., 1986; Beach et al., 2012; Braak and Braak, 1990; Rudelli et al., 1984). Higher plaque accumulation in the striatum was highly sensitive (95.8%) and moderately (75.7%) specific to Braak neurofibrillary tangle stage V or VI. Furthermore, a higher striatal plaque density score had 85.6% sensitivity and 86.2% specificity for the presence of dementia and clinicopathological AD (Beach et al., 2012). The parahippocampal

gyrus is located in an MTL region that projects onto the hippocampus and is activated during olfactory encoding, working memory, and successful recognition memory (Cerf-Ducastel and Murphy, 2009; Haase et al., 2013; Luzzi et al., 2007; Stoub et al., 2006). The isthmus of the cingulate gyrus connects the cingulate gyrus to the parahippocampal gyrus and has shown long-term volume reduction in response to stressful life events and dementia within older populations (Calati et al., 2018; Sener, 1997; Yang et al., 2016).

Females demonstrated significantly greater thickness measurements in the left parahippocampal gyrus, relative to males ($M_F = 2.56$ vs. $M_M = 2.21$; $p = 0.004$). The ε_4 carrier group, relative to the ε_4 non-carriers, demonstrated significantly larger volumes in the left putamen ($M_+ = 5216.33$ vs. $M_- = 4668.43$; $p = 0.03$) and right putamen ($M_+ = 5154.44$ vs. $M_- = 4412.14$; $p = 0.002$).

The ε_4 status × sex interaction effect was also significant ($p = 0.041$; Fig. 2). When simple effects were examined, male ε_4 non-carriers demonstrated significantly greater thickness measurements relative to male ε_4 carriers ($M_{M-} = 2.666$ vs. $M_{M+} = 2.359$; $p = 0.002$).

3.5.2. Post hoc partial correlation analyses—

We performed partial correlational analyses, controlling for age and ICV, between neuroimaging data and DRS scores using the same methods described in Section 2.4.4. We found a significant, positive association between DRS scores and functional activation in the right parahippocampal gyrus during FPs in male ε_4 carriers ($r = 0.952$, $p = 0.003$; Fig. 3).

4. Discussion

4.1. Structural neuroimaging

Our first hypothesis, that ε_4 carriers would demonstrate smaller volumetric and thickness measurements in memory regions relative to ε_4 non-carriers, was not upheld. We found that ε_4 carriers demonstrated significantly larger bilateral putamen volumes. The larger volumetric measurements may be related to inflammation, plaque accumulation, and shape abnormalities previously associated with striatal areas (Beach et al., 2012; Braak and Braak, 1990; de Jong et al., 2008, 2011; Pievani et al., 2013; Rudelli et al., 1984). Inflammation and Aβ plaque accumulation have been suggested as possible explanations for increased thickness or volumetric measurements (Fox et al., 2005). An fluorodeoxyglucose (FDG)-positron emission tomography (PET) study found that the putamen of cognitively normal ApoE ε_4 homozygotes had the highest amyloid deposition relative to other brain regions (Pardo and Lee, 2018). Similarly, another fluorodeoxyglucose (FDG)-positron emission tomography (PET) study found that amyloid deposition occurs very early in the striatum, which is comprised of the caudate and putamen, and these deposits are often not associated with clinical symptoms (Klunk et al., 2007). Furthermore, an X-ray micro-diffraction study demonstrated that there can be structural heterogeneity of amyloid such that subjects with different clinical histories may contain different ensembles of fibrillar structures (Liu et al., 2016). Polymorphism in the distribution of amyloid in plaques may be related to different disease states and variable manifestations of clinical symptoms (Liu et al., 2016; Lu et al., 2013).

The greater putamen volumes may also be attributed to neuronal compensation, which refers to a dissociation between brain pathology and behavioral change during the early and prodromal stages of neurodegenerative diseases (Gregory et al., 2017; Scheller et al., 2014). It has been proposed that in conjunction with pathological loss of brain tissue, there is a structural reorganization in the brain to compensate for these losses, which enables prodromal patients to perform functionally at the same level as those not at risk for AD (Gregory et al., 2017). It is the lack of behavioral differences between groups that indicates neuronal compensation (Gregory et al., 2017). Task performance data suggest that there were no differences between ε_4 carriers and non-carriers, except for run 1, when ε_4 carriers made *more* hits relative to ε_4 non-carriers. Larger putamen volumes have also been found in other developmental or neurodegenerative disorders. When adults with autism spectrum disorder and typical developed controls were compared, the putamen was found to be significantly larger in the autism spectrum disorder group after controlling for age, sex, and ICV (Sato et al., 2014). Similarly, larger putamen volumes have been reported in individuals with bipolar disorder, schizophrenia, and obsessive-compulsive disorders (Luo et al., 2019). Hyperactivation in dopamine pathways within the striatum has been suggested to be the cause of this enlargement of the dopamine-rich putamen (Luo et al., 2019). We therefore suspect that the greater putamen volumes may be indicative of overcompensation which allows ε_4 carriers to maintain functional performance in response to changes imposed by aging and ε_4 status.

We found sex effects on thickness measurements in the left parahippocampal gyrus and left isthmus cingulate. Increasing asymmetry in these regions is associated with the transition of mild cognitive impairment (MCI) to AD (Long et al., 2013). A recent longitudinal study reported that when comparing ε_4 carriers and ε_4 non-carriers, ε_4 carriers demonstrated greater rates of volume loss in the hippocampus and parahippocampal gyrus (Reiter et al., 2017). The isthmus cingulate, which connects the cingulate gyrus to the parahippocampal gyrus, was significantly reduced in ε_4 carriers and in male ε_4 carriers relative to ε_4 non-carriers and male ε_4 non-carriers, respectively (Sener,1997). This finding is supported by previous literature reporting greater atrophy and increased rate of cortical thinning in the isthmus cingulate in AD (Hayata et al., 2015; Mak et al., 2015; Vasconcelos et al., 2014).

4.2. Functional neuroimaging

Our second hypothesis, that ε_4 carriers would demonstrate less functional activation during hits and greater functional activation during FPs, was partially upheld. Furthermore, we hypothesized that this activation would be especially pronounced in male ε_4 carriers; this was strongly upheld. The ε_4 carrier group, relative to ε_4 non-carriers, and male ε_4 carriers, relative to female ε_4 carriers, showed greater recruitment during FPs and hits, respectively in brain regions associated with memory and decision-making (e.g., BA10, precuneus, PCC, ACC). The BA10 is an area associated with encoding the incentive value of a stimulus during decision-making and is activated by a reward stimulus when already activated by working memory processing (O'Doherty et al., 2001). The precuneus is an integral region associated with source memory retrieval and the PCC demonstrates activation during autobiographical memory retrieval (Bonnì et al., 2015; Maddock et al., 2001). Lateralization

in the ACC has been activated in error processing and conflict monitoring, suggesting that the ACC is vital in making correct choices (Lütcke and Frahm, 2008).

The precuneus and PCC are not only associated with memory and information processing, but also affected early in AD progression. Hyperactivation in the left precuneus and right cingulate gyrus was found in early AD patients, relative to healthy controls, during a time representation task (Leyhe et al., 2009). During a semantic memory task, increased activation in the bilateral PCC and precuneus has been reported in asymptomatic ε_4 carriers relative to controls (Seidenberg et al., 2009). Atrophy in tracts connecting the hippocampus to the precuneus and PCC differentiates normal controls from MCI and AD patients (Palesi et al., 2012). Furthermore, abnormal hypoperfusion in the PCC and precuneus distinguishes MCI patients from normal controls (Bradley et al., 2002; Rombouts et al., 2005).

It is noteworthy that despite no significant differences in FP rates, ε_4 carriers demonstrated significantly greater cognitive expenditure during FPs when compared to non-carriers. Hyperactivation has been previously noted in AD populations and is often understood as a compensatory response to functional impairment and accumulating AD pathology, possibly even acting as a protective factor to help ε_4 carriers maintain their cognitive abilities in the short-term (Dickerson et al., 2004; Leyhe et al., 2009; Seidenberg et al., 2009; Woodard et al., 2010). This compensatory response may occur to support task performance in response to reduced communication between brain regions that typically function together (Seidenberg et al., 2009; Zhu et al., 2015). Age-related activation increases have been correlated with poorer behavioral performance and lower white matter integrity (Zhu et al., 2015). Furthermore, excessive hyperactivation over time can lead to excitotoxicity and ultimately result in synapse degeneration and death (Mattson and Chan, 2003; Poirier et al., 1993; Woodard et al., 2010; Yanker, 1996) and has been suggested as one mechanism contributing to olfactory dysfunction in AD (Jacobson et al., 2019; Murphy, 2019). Interestingly, ApoE ε_4 carrier mice show hyperactivation in olfactory areas that has been associated with olfactory deficits, suggesting that subtle, early olfactory deficits may presage future abnormalities in olfactory circuitry, and further supporting the hypothesis that hyperactivation is associated with olfactory dysfunction (East et al., 2018; Peng et al., 2017). This hyperactivation has been suggested to precede clinical symptoms in the AD pathological timeline (Gregory et al., 2017; Murphy, 2019).

4.3. Partial correlations: neuroimaging data

The third hypothesis, that neuroimaging data and DRS scores would be associated in all groups, was partially upheld. Partial correlations revealed significant associations between neuroimaging data and DRS scores within males. For male ε_4 carriers, activation in the right parahippocampal gyrus was associated with higher DRS scores after age, ICV, and right parahippocampal gyrus thickness were partialed out. Higher DRS scores suggest greater global cognitive functioning (Mattis, 1998). These results support the hypothesis that hyperactivation may be protective against cognitive decline in the short term. In the male ε_4 non-carrier group, larger right hippocampal volume was associated with lower DRS scores after controlling for age and ICV. This association suggests that within this sample, greater right hippocampal volume does not necessarily mean better global cognitive functioning.

5. Conclusions

The present study is the first to investigate how the interaction of sex and ApoE ε_4 status impacts both structural MRI and fMRI activation during an olfactory recognition memory task in a non-demented, older population. The study demonstrates differential neuroimaging data and olfactory memory processing in relation to sex and ApoE ε_4 status. No study to our knowledge has reported both structural and functional neuroimaging data within older, non-demented ε_4 carriers and non-carriers during an olfactory recognition memory task. Moreover, neuroimaging studies reporting on sex differences present in olfactory recognition memory processing are lacking. Our results expand preceding literature suggesting hyperactivation patterns in those at risk for AD and provide valuable information regarding structural differences between ε_4 carriers and ε_4 non-carriers before AD symptoms manifest. Results suggest that prior to developing AD symptomatology, male ε_4 carriers demonstrate hyperactivation during odor recognition memory relative to other groups, which may ultimately lead to future brain atrophy and decreased cognitive functioning.

There were limitations to our study. First, the study would have benefitted from larger sample sizes. Although we considered structural neuroimaging data and fMRI, we did not include data on amyloid and plaque accumulation through other imaging methods (e.g., amyloid-PET imaging, diffusion tensor imaging), which allow for examination of pre-mortem amyloid plaque burden (Hedden et al., 2013; Klunk et al., 2004). Future studies may consider these methods in conjunction with fMRI and structural MRI.

Together, our findings underscore the potential of incorporating MRI methodologies, genetics, and sex differences to identify those at risk for AD. As clinical trial research progresses to develop measures or interventions intended to slow or prevent AD clinical progression, it is imperative that we consider these factors to design interventions that are suitable, effective, and most beneficial for the population.

Supplementary Material

Refer to Web version on PubMed Central for supplementary material.

Acknowledgements

This study is supported by the National Institutes of Health (grant numbers R01AG004085-26 and R01AG062006-01) from the National Institute on Aging (to C.M.). This content is solely the responsibility of the authors and does not necessarily represent the official views of the granting agency. We would like to thank the members of the Lifespan Human Senses Laboratory for all of their assistance, especially Aaron Jacobson, Lori Haase, Erin Green, MiRan Wang, and Vincent Rupp for their contributions to data collection and analysis. We gratefully acknowledge the assistance of Dr Thomas Liu and the UCSD Center for fMRI.

References

Albers AD, Asafu-Adjei J, Delaney MK, Kelly KE, Gomez-Isla T, Blacker D, Albers MW, 2016 Episodic memory of odors stratifies Alzheimer biomarkers in normal elderly. Ann. Neurol 80, 846–857. [PubMed: 27696605]

Albers MW, Gilmore GC, Kaye J, Murphy C, Wingfield A, Bennett DA, Zhang LI, 2015 At the interface of sensory and motor dysfunctions and Alzheimer's disease. Alzheimers Dement. 11, 70–98. [PubMed: 25022540]

Alexander GE, DeLong MR, Strick PL, 1986 Parallel organization of functionally segregated circuits linking basal ganglia and cortex. Annu. Rev. Neurosci 9, 357–381. [PubMed: 3085570]

Altmann A, Tian L, Henderson VW, Greicius MD, 2014 Sex modifies the APOE-related risk of developing Alzheimer's disease. Ann. Neurol 75, 563–573. [PubMed: 24623176]

Alzheimer's Association, 2018 2018 Alzheimer's disease facts and figures. Alzheimers Dement. 14, 367–429.

Attems J, Lintner F, Jellinger KA, 2005 Olfactory involvement in aging and Alzheimer's disease: an autopsy study. J. Alzheimers Dis 7, 149–157. [PubMed: 15851853]

Attems J, Neltner JH, Nelson PT, 2014 Quantitative neuropathological assessment to investigate cerebral multi-morbidity. Alzheimers Res. Ther 6, 1–8. [PubMed: 24382028]

Bartrés-Faz D, Junqué C, Moral P, Lopez-Aldomar A, Sanchez-Aldeguer J, Clemente IC, 2002 Apolipoprotein E gender effects on cognitive performance in age-associated memory impairment. J. Neuropsychiatry Clin. Neurosci 14, 80–83. [PubMed: 11884660]

Beach TG, Sue LI, Walker DG, Sabbagh MN, Serrano G, Dugger B, Souders L, 2012 Striatal amyloid plaque density predicts Braak neurofibrillary stage and clinicopathological Alzheimer's disease: implications for amyloid imaging. J. Alzheimers Dis 28, 869–876. [PubMed: 22112552]

Blennow K, de Leon MJ, Zetterberg H, 2006 Alzheimer's disease. Lancet 368, 387–403. [PubMed: 16876668]

Bonnì S, Veniero D, Mastropasqua C, Ponzo V, Caltagirone C, Bozzali M, Koch G, 2015 TMS evidence for a selective role of the precuneus in source memory retrieval. Behav. Brain Res 282, 70–75. [PubMed: 25541040]

Braak H, Braak E, 1990 Alzheimer's disease: striatal amyloid deposits and neurofibrillary changes. J. Neuropathol. Exp. Neurol 49, 215–224. [PubMed: 1692337]

Braak H, Braak E, 1996 Evolution of the neuropathology of Alzheimer's disease. Acta Neurol. Scand 94, 3–12.

Braak H, Braak E, 1997 Frequency of stages of Alzheimer-related lesions in different age categories. Neurobiol. Aging 18, 351–357. [PubMed: 9330961]

Braak H, Braak E, 1991 Neuropathological stageing of Alzheimer-related changes. Acta Neuropathol. 82, 239–259. [PubMed: 1759558]

Bradley KM, O'Sullivan VT, Soper NDW, Nagy Z, King EM-F, Smith AD, Shepstone BJ, 2002 Cerebral perfusion SPET correlated with Braak pathological stage in Alzheimer's disease. Brain 125, 1772–1781. [PubMed: 12135968]

Bu G, 2009 Apolipoprotein E and its receptors in Alzheimer's disease: pathways, pathogenesis and therapy. Nat. Rev. Neurosci 10, 333–344. [PubMed: 19339974]

Calati R, Maller JJ, Meslin C, Lopez-Castroman J, Ritchie K, Courtet P, Artero S, 2018 Repatriation is associated with isthmus cingulate cortex reduction in community-dwelling elderly. World J. Biol. Psychiatry 19, 421–430. [PubMed: 27844618]

Calhoun-Haney R, Murphy C, 2005 Apolipoprotein ε4 is associated with more rapid decline in odor identification than in odor threshold or Dementia Rating Scale scores. Brain Cogn. 58, 178–182. [PubMed: 15919549]

Cerf-Ducastel B, Murphy C, 2009 Age-related differences in the neural substrates of cross-modal olfactory recognition memory: an fMRI investigation. Brain Res. 1285, 1–20. [PubMed: 19524556]

Cerf-Ducastel B, Murphy C, 2006 Neural substrates of cross-modal olfactory recognition memory: an fMRI study. Neuroimage 31, 386–396. [PubMed: 16414279]

Chen J, Shu H, Wang Z, Liu D, Shi Y, Xu L, Zhang Z, 2016 Protective effect of APOE epsilon 2 on intrinsic functional connectivity of the entorhinal cortex is associated with better episodic memory in elderly individuals with risk factors for Alzheimer's disease. Oncotarget 7, 58789–58801. [PubMed: 27542235]

Chen Y, Chen K, Zhang J, Li X, Shu N, Wang J, Reiman EM, 2015 Disrupted functional and structural networks in cognitively normal elderly subjects with the APOE ε4 allele. Neuropsychopharmacology 40, 1181–1191. [PubMed: 25403724]

Cox RW, 1996 AFNI: software for analysis and visualization of functional magnetic resonance neuroimages. Comput. Biomed. Res 29, 162–173. [PubMed: 8812068]

Cox RW, Hyde JS, 1997 Software tools for analysis and visualization of FMRI data. NMR Biomed. 10, 171–178. [PubMed: 9430344]

Dale AM, Fischl B, Sereno MI, 1999 Cortical surface-based analysis. I. Segmentation and surface reconstruction. Neuroimage 9, 179–194. [PubMed: 9931268]

Dale AM, Sereno MI, 1993 Improved localization of cortical activity by combining EEG and MEG with MRI cortical surface reconstruction: a linear approach. J. Cogn. Neurosci 5, 162–176. [PubMed: 23972151]

de Jong LW, Ferrarini L, Van der Grond J, Milles JR, Reiber JHC, Westendorp RGJ, Buchem M.A. van., 2011 Shape abnormalities of the striatum in Alzheimer's disease. J. Alzheimers Dis 23, 49–59. [PubMed: 20930298]

de Jong LW, van der Hiele K, Veer IM, Houwing JJ, Westendorp RGJ, Bollen ELEM, van der Grond J, 2008 Strongly reduced volumes of putamen and thalamus in Alzheimer's disease: an MRI study. Brain 131, 3277–3285. [PubMed: 19022861]

Desikan RS, Ségonne F, Fischl B, Quinn BT, Dickerson BC, Blacker D, Killiany RJ, 2006 An automated labeling system for subdividing the human cerebral cortex on MRI scans into gyral based regions of interest. Neuroimage 31, 968–980. [PubMed: 16530430]

Dickerson BC, Salat DH, Bates JF, Atiya M, Killiany RJ, Greve DN, Sperling RA, 2004 Medial temporal lobe function and structure in mild cognitive impairment. Ann. Neurol 56, 27–35. [PubMed: 15236399]

Dowell NG, Evans SL, Tofts PS, King SL, Tabet N, Rusted JM, 2016 Structural and resting-state MRI detects regional brain differences in young and mid-age healthy APOE-e4 carriers compared with non-APOE-e4 carriers. NMR Biomed. 29, 614–624. [PubMed: 26929040]

East BS, Fleming G, Peng K, Olofsson JK, Levy E, Mathews PM, Wilson DA, 2018 Human apolipoprotein E genotype differentially affects olfactory behavior and sensory physiology in mice. Neuroscience 1, 103–110.

Esiri MM, Wilcock GK, 1984 The olfactory bulbs in Alzheimer's disease. J. Neurol. Neurosurg. Psychiatry 47, 56–60. [PubMed: 6693914]

Farrer LA, Cupples LA, Haines JL, Hyman B, Kukull WA, Mayeux R, van Dujin CM, 1997 Effects of age, sex, and ethnicity on the association between apolipoprotein E genotype and Alzheimer disease: a meta-analysis. JAMA 278, 1349. [PubMed: 9343467]

Filippini N, MacIntosh BJ, Hough MG, Goodwin GM, Frisoni GB, Smith SM, Mackay CE, 2009 Distinct patterns of brain activity in young carriers of the APOE-4 allele. Proc. Natl. Acad. Sci. U. S. A 106, 7209–7214. [PubMed: 19357304]

Fischl B, Dale AM, 2000 Measuring the thickness of the human cerebral cortex from magnetic resonance images. Proc. Natl. Acad. Sci. U. S. A 97, 11050–11055. [PubMed: 10984517]

Fischl B, Liu A, Dale AM, 2001 Automated manifold surgery: constructing geometrically accurate and topologically correct models of the human cerebral cortex. IEEE Trans. Med. Imaging 20, 70–80. [PubMed: 11293693]

Fischl B, Salat DH, Busa E, Albert M, Dieterich M, Haselgrove C, Dale AM, 2002 Whole brain segmentation. Neuron 33, 341e355.

Fischl B, Salat DH, van der Kouwe AJW, Makris N, Ségonne F, Quinn BT, Dale AM, 2004a Sequence-independent segmentation of magnetic resonance images. Neuroimage 23, S69–S84. [PubMed: 15501102]

Fischl B, Sereno MI, Dale AM, 1999a Cortical surface-based analysis II: inflation, flattening, and a surface-based coordinate system. Neuroimage 9, 195–207. [PubMed: 9931269]

Fischl B, Sereno MI, Tootell RB, Dale AM, 1999b High-resolution intersubject averaging and a coordinate system for the cortical surface. Hum. Brain Mapp 8, 272–284. [PubMed: 10619420]

Fischl B, van der Kouwe A, Destrieux C, Halgren E, Segonne F, Salat DH, Busa E, Seidman LJ, Goldstein J, Kennedy D, Caviness V, Makris N, Rosen B, Dale AM, 2004b Automatically parcellating the human cerebral cortex. Cereb. Cortex 14, 11–22. [PubMed: 14654453]

Fox NC, Black RS, Gilman S, Rossor MN, Griffith SG, Jenkins L, for the AN1792(QS-21)-201 Study Team, 2005 Effects of Ab immunization (AN1792) on MRI measures of cerebral volume in Alzheimer disease. Neurology 64, 1563–1572. [PubMed: 15883317]

Frisoni GB, Fox NC, Jack CR, Scheltens P, Thomson PM, 2010 The clinical use of structural MRI in Alzheimer disease. Nat. Rev. Neurol 6, 67–77. [PubMed: 20139996]

Gilbert PE, Murphy C, 2004 The effect of the ApoE ε4 allele on recognition memory for olfactory and visual stimuli in patients with pathologically confirmed Alzheimer's disease, probable Alzheimer's disease, and healthy elderly controls. J. Clin. Exp. Neuropsychol 26, 779–794. [PubMed: 15370375]

Gold S, Christian B, Arndt S, Zeien G, Cizadlo T, Johnson DL, Flaum M, Andreasen NC, 1998 Functional MRI statistical software packages: a comparative analysis. Hum. Brain Mapp 6, 73–84. [PubMed: 9673664]

Gregory S, Long JD, Klöppel S, Razi A, Scheller E, Minkova L, Rees G, 2017 Operationalizing compensation over time in neurodegenerative disease. Brain 140, 1158–1165. [PubMed: 28334888]

Haase L, Wang M, Green E, Murphy C, 2013 Functional connectivity during recognition memory in individuals genetically at risk for Alzheimer's disease.Hum. Brain Mapp. 34, 530–542.

Han X, Jovicich J, Salat D, van der Kouwe A, Quinn B, Czanner S, Busa E, Pacheco J, Albert M, Killiany R, Maguire P, Rosas D, Makris N, Dale A, Dickerson B, Fischl B, 2006 Reliability of MRI-derived measurements of human cerebral cortical thickness: the effects of field strength, scanner upgrade and manufacturer. Neuroimage 32, 180–194. [PubMed: 16651008]

Hayata TT, Bergo FPG, Rezende TJ, Damasceno A, Damasceno BP, Cendes F, Balthazar MLF, 2015 Cortical correlates of affective syndrome in dementia due to Alzheimer's disease. Arq. Neuropsiquiatr 73, 553–560. [PubMed: 26200048]

Hedden T, Oh H, Younger AP, Patel TA, 2013 Meta-analysis of amyloidcognition relations in cognitively normal older adults. Neurology 80, 1341–1348. [PubMed: 23547267]

Holland D, Desikan RS, Dale AM, McEvoy LK, 2013 Higher rates of decline for women and apolipoprotein E ε4 carriers. Am. J. Neuroradiol 34, 2287–2293. [PubMed: 23828104]

Hyman BT, 1997 The neuropathological diagnosis of Alzheimer's disease: clinicalpathological studies. Neurobiol. Aging 18, S27–S32. [PubMed: 9330982]

Hyman BT, Gomez-Isla T, Briggs M, Chung H, Nichols S, Kohout F, Wallace R, 1996 Apolipoprotein E and cognitive change in an elderly population. Ann. Neurol 40, 55–66. [PubMed: 8687193]

Jacobson A, Green E, Haase L, Szajer J, Murphy C, 2019 Differential effects of BMI on brain response to odor in olfactory, reward and memory regions: evidence from fMRI. Nutrients 11, 926.

Jovicich J, Czanner S, Greve D, Haley E, van der Kouwe A, Gollub R, Kennedy D, Schmitt F, Brown G, Macfall J, Fischl B, Dale A, 2006 Reliability in multi-site structural MRI studies: effects of gradient non-linearity correction on phantom and human data. Neuroimage 30, 436–443. [PubMed: 16300968]

Klunk WE, Engler H, Nordberg A, Wang Y, Blomqvist G, Holt DP, Långström B, 2004 Imaging brain amyloid in Alzheimer's disease with Pittsburgh Compound-B. Ann. Neurol 55, 306–319. [PubMed: 14991808]

Klunk WE, Price JC, Mathis CA, Tsopelas ND, Lopresti BJ, Ziolko SK, DeKosky ST, 2007 Amyloid deposition begins in the striatum of presenilin-1 mutation carriers from two unrelated pedigrees. J. Neurosci 27, 6174–6184. [PubMed: 17553989]

Kuperberg GR, Broome MR, McGuire PK, David AS, Eddy M, Ozawa F, Williams SCR, 2003 Regionally localized thinning of the cerebral cortex in schizophrenia. Arch. Gen. Psychiatry 60, 11.

Leyhe T, Erb M, Milian M, Eschweiler GW, Ethofer T, Grodd W, Saur R, 2009 Changes in cortical activation during retrieval of clock time representations in patients with mild cognitive impairment and early Alzheimer's disease. Dement. Geriatr. Cogn. Disord. 27, 117–132. [PubMed: 19182479]

Lind J, Persson J, Ingvar M, Larsson A, Cruts M, Van Broeckhoven C, Nyberg L, 2006 Reduced functional brain activity response in cognitively intact apolipoprotein E ε4 carriers. Brain 129, 1240–1248. [PubMed: 16537568]

Liu J, Costantino I, Venugopalan N, Fischetti RF, Hyman BT, Frosch MP, Makowski L, 2016 Amyloid structure exhibits polymorphism on multiple length scales in human brain tissue. Sci. Rep 6.

Long X, Zhang L, Liao W, Jiang C, Qiu B, 2013 Distinct laterality alterations distinguish mild cognitive impairment and Alzheimer's disease from healthy aging: statistical parametric mapping with high resolution MRI. Hum. Brain Mapp 34, 3400–3410. [PubMed: 22927141]

Lu J-X, Qiang W, Yau W-M, Schwieters CD, Meredith SC, Tycko R, 2013 Molecular structure of b-amyloid fibrils in Alzheimer's disease brain tissue. Cell 154, 1257–1268. [PubMed: 24034249]

Luo X, Mao Q, Shi J, Wang X, Li C-SR, 2019 Putamen gray matter volumes in neuropsychiatric and neurodegenerative disorders. World J. Psychiatry Ment. Health Res 3.

Lütcke H, Frahm J, 2008 Lateralized anterior cingulate function during error processing and conflict monitoring as revealed by high-resolution fMRI. Cereb. Cortex 18, 508–515. [PubMed: 17576750]

Luzzi S, Snowden JS, Neary D, Coccia M, Provinciali L, Lambon Ralph MA, 2007 Distinct patterns of olfactory impairment in Alzheimer's disease, semantic dementia, frontotemporal dementia, and corticobasal degeneration. Neuropsychologia 45, 1823–1831. [PubMed: 17270222]

Maddock RJ, Garrett AS, Buonocore MH, 2001 Remembering familiar people: the posterior cingulate cortex and autobiographical memory retrieval. Neuroscience 104, 667–676. [PubMed: 11440800]

Mahley RW, Huang Y, 2012 Apolipoprotein E sets the stage: response to injury triggers neuropathology. Neuron 76, 871–885. [PubMed: 23217737]

Mahley RW, Rall SC, 2000 Apolipoprotein E: far more than a lipid transport protein. Annu. Rev. Genomics Hum. Genet 1, 507–537. [PubMed: 11701639]

Mak E, Su L, Williams GB, Watson R, Firbank MJ, Blamire AM, O'Brien JT, 2015 Progressive cortical thinning and subcortical atrophy in dementia with Lewy bodies and Alzheimer's disease. Neurobiol. Aging 36, 1743–1750. [PubMed: 25649023]

Mattis S, 1988 Dementia Rating Scale (DRS) Professional Manual. Psychological Assessment Resources, Inc, Odessa, FL.

Mattson MP, Chan SL, 2003 Neuronal and glial calcium signaling in Alzheimer's disease. Cell Calcium 34, 385–397. [PubMed: 12909083]

Moberg PJ, Pearlson GD, Speedie LJ, Lipsey JR, Strauss ME, Folstein SE, 1987 Olfactory recognition: differential impairments in early and late Huntington's and Alzheimer's diseases. J. Clin. Exp. Neuropsychol 9, 650–664. [PubMed: 2961789]

Mondadori CRA, de Quervain DJ-F, Buchmann A, Mustovic H, Wollmer MA, Schmidt CF, Henke K, 2007 Better memory and neural efficiency in young apolipoprotein E 4 carriers. Cereb. Cortex 17, 1934–1947. [PubMed: 17077159]

Murphy C, 2019 Olfactory and other sensory impairments in Alzheimer disease. Nat. Rev. Neurol 15, 11–24. [PubMed: 30532084]

Murphy C, Gilmore MM, Seery CS, Salmon DP, Lasker BR, 1990 Olfactory thresholds are associated with degree of dementia in Alzheimer's disease. Neurobiol. Aging 11, 465–469. [PubMed: 2381506]

Murphy C, Jernigan TL, Fennema-Notestine C, 2003 Left hippocampal volume loss in Alzheimer's disease is reflected in performance on odor identification: a structural MRI study. J. Int. Neuropsychol. Soc 9.

Murphy C, Nordin S, Acosta L, 1997 Odor learning, recall, and recognition memory in young and elderly adults. Neuropsychology 11, 126–137. [PubMed: 9055276]

Murphy C, Nordin S, Jinich S, 1999 Very early decline in recognition memory for odors in Alzheimer's disease. Aging Neuropsychol. Cogn 6, 229–240.

Murphy C, Schubert CR, Cruickshanks KJ, Klein BEK, Klein R, Nondahl DM, 2002 Prevalence of olfactory impairment in older adults. JAMA 288, 2307. [PubMed: 12425708]

Nordin S, Murphy C, 1996 Impaired sensory and cognitive olfactory function in questionable Alzheimer's disease. Neuropsychology 10, 113–119.

Nordin S, Murphy C, 2006 Odor memory in normal aging and Alzheimer's disease. Ann. N. Y. Acad. Sci 855, 686–693.

O'Doherty J, Kringelbach ML, Rolls ET, Hornak J, Andrews C, 2001 Abstract reward and punishment representations in the human orbitofrontal cortex. Nat. Neurosci 4, 95–102. [PubMed: 11135651]

Olofsson JK, Nordin S, Wiens S, Hedner M, Nilsson L-G, Larson M, 2010 Odor identification impairment in carriers of ApoE-e4 is independent of clinical dementia. Neurobiol. Aging 31, 567–577. [PubMed: 18619712]

Palesi F, Vitali P, Chiarati P, Castellazzi G, Caverzasi E, Pichiecchio A, Bastianello S, 2012 DTI and MR volumetry of hippocampus-PC/PCC circuit: in search of early micro- and macrostructural signs of Alzheimer's disease. Neurol. Res. Int 2012, 1–9.

Pardo JV, Lee JT, 2018 Atypical localization and dissociation between glucose uptake and amyloid deposition in cognitively normal APOE*E4 homozygotic elders compared with patients with late-onset Alzheimer's disease. eNeuro 5.

Payami H, Zareparsi S, Montee KR, Sexton GJ, Kaye JA, Bird TD, Schellenberg GD, 1996 Gender difference in apolipoprotein E-associated risk for familial Alzheimer disease: a possible clue to the higher incidence of Alzheimer disease in women. Am. J. Hum. Genet 58, 803–811. [PubMed: 8644745]

Peng KY, Mathews PM, Levy E, Wilson DA, 2017 Apolipoprotein E4 causes early olfactory network abnormalities and short-term olfactory memory impairments. Neuroscience 20, 364–371.

Pievani M, Bocchetta M, Boccardi M, Cavedo E, Bonetti M, Thompson PM, Frisoni GB, 2013 Striatal morphology in early-onset and late-onset Alzheimer's disease: a preliminary study. Neurobiol. Aging 34, 1728–1739. [PubMed: 23428181]

Poirier J, Bertrand P, Poirier J, Kogan S, Gauthier S, Poirier J, Davignon J, 1993 Apolipoprotein E polymorphism and Alzheimer's disease. Lancet 342, 697–699. [PubMed: 8103819]

Price JL, Davis PB, Morris JC, White DL, 1991 The distribution of tangles, plaques and related immunohistochemical markers in healthy aging and Alzheimer's disease. Neurobiol. Aging 12, 295–312. [PubMed: 1961359]

Reiter K, Nielson KA, Durgerian S, Woodard JL, Smith JC, Seidenberg M, Rao SM, 2017 Five-year longitudinal brain volume change in healthy elders at genetic risk for Alzheimer's disease. J. Alzheimers Dis 55, 1363–1377. [PubMed: 27834774]

Reuter M, Fischl B, 2011 Avoiding asymmetry-induced bias in longitudinal image processing. Neuroimage 57, 19–21. [PubMed: 21376812]

Reuter M, Rosas HD, Fischl B, 2010 Highly accurate inverse consistent registration: a robust approach. Neuroimage 53, 1181–1196. [PubMed: 20637289]

Reuter M, Schmansky NJ, Rosas HD, Fischl B, 2012 Within-subject template estimation for unbiased longitudinal image analysis. Neuroimage 61, 1402–1418. [PubMed: 22430496]

Rombouts SARB, Barkhof F, Goekoop R, Stam CJ, Scheltens P, 2005 Altered resting state networks in mild cognitive impairment and mild Alzheimer's disease: an fMRI study. Hum. Brain Mapp 26, 231–239. [PubMed: 15954139]

Rosas HD, Liu AK, Hersch S, Glessner M, Ferrante RJ, Salat DH, van der Kouwe A, Jenkins BG, Dale AM, Fischl B, 2002 Regional and progressive thinning of the cortical ribbon in Huntington's disease. Neurology 58, 695–701. [PubMed: 11889230]

Rudelli RD, Ambler MW, Wisniewski HM, 1984 Morphology and distribution of Alzheimer neuritic (senile) and amyloid plaques in striatum and diencephalon. Acta Neuropathol. 64, 273–281. [PubMed: 6542292]

Salat DH, Buckner RL, Snyder AZ, Greve DN, Desikan RSR, Busa E, Fischl B, 2004 Thinning of the cerebral cortex in aging. Cereb. Cortex 14, 721–730. [PubMed: 15054051]

Sato W, Kubota Y, Kochiyama T, Uono S, Yoshimura S, Sawada R, Toichi M, 2014 Increased putamen volume in adults with autism spectrum disorder. Front. Hum. Neurosci 8.

Scheller E, Minkova L, Leitner M, Klöppel S, 2014 Attempted and successful compensation in preclinical and early manifest neurodegenerationda review of task fMRI studies. Front. Psychiatry 5.

Ségonne F, Dale AM, Busa E, Glessner M,Salat D, Hahn HK, Fischl B, 2004 A hybrid approach to the skull stripping problem in MRI. Neuroimage 22, 1060–1075. [PubMed: 15219578]

Ségonne F, Pacheco J, Fischl B, 2007 Geometrically accurate topology-correction of cortical surfaces using nonseparating loops. IEEE Trans. Med. Imaging 26, 518–529. [PubMed: 17427739]

Seidenberg M, Guidotti L, Nielson KA, Woodard JL, Durgerian S, Antuono P, Rao SM, 2009 Semantic memory activation in individuals at risk for developing Alzheimer disease. Neurology 73, 612–620. [PubMed: 19704080]

Sener RN, 1997 Large isthmus of the cingulate gyrus: an unusual anatomical variation simulating tumor. Comput. Med. Imaging Graph 21, 337–339. [PubMed: 9690006]

Ship JA, Pearson JD, Cruise LJ, Brant LJ, Metter EJ, 1996 Longitudinal changes in smell identification. J. Gerontol. A. Biol. Sci. Med. Sci 51A, M86–M91.

Sled JG, Zijdenbos AP, Evans AC, 1998 A nonparametric method for automatic correction of intensity nonuniformity in MRI data. IEEE Trans. Med. Imaging 17, 87–97. [PubMed: 9617910]

Smith SM, Jenkinson M, Woolrich MW, Beckmann CF, Behrens TEJ, Johansen-Berg H, Matthews PM, 2004 Advances in functional and structural MR image analysis and implementation as FSL. Neuroimage 23, S208–S219. [PubMed: 15501092]

Stark CEL, Squire LR, 2000a FMRI activity in the medial temporal lobe during recognitionmemoryasafunctionofstudy-testinterval. Hippocampus 10,329–337. [PubMed: 10902902]

Stark CEL, Squire LR, 2000b Functional magnetic resonance imaging (fMRI) activity in the hippocampal region during recognition memory. J. Neurosci 20, 7776–7781. [PubMed: 11027241]

Stoub TR, deToledo-Morrell L, Stebbins GT, Leurgans S, Bennett DA, Shah RC, 2006 Hippocampal disconnection contributes to memory dysfunction in individuals at risk for Alzheimer's disease. Proc. Natl. Acad. Sci. U. S. A 103, 10041–10045. [PubMed: 16785436]

Ungar L, Altmann A, Greicius MD, 2014 Apolipoprotein E, gender, and Alzheimer's disease: an overlooked, but potent and promising interaction. Brain Imaging Behav. 8, 262–273. [PubMed: 24293121]

Vasconcelos L. de G, Jackowski AP, de Oliveira MO, Flor YMR, Souza AAL, Bueno OFA, Brucki SMD, 2014 The thickness of posterior cortical areas is related to executive dysfunction in Alzheimer's disease. Clinics 69, 28–37.

Visser P, Verhey F, Hofman P, Scheltens P, Jolles J, 2002 Medial temporal lobe atrophy predicts Alzheimer's disease in patients with minor cognitive impairment. J. Neurol. Neurosurg. Psychiatry 72, 491–497. [PubMed: 11909909]

Wehling EI, Lundervold AJ, Nordin S, Wollschlaeger D, 2016 Longitudinal changes in familiarity, free and cued odor identification, and edibility judgments for odors in aging individuals. Chem. Senses 41, 155–161. [PubMed: 26547014]

Woodard JL, Seidenberg M, Nielson KA, Smith JC, Antuono P, Durgerian S, Rao SM, 2010 Prediction of cognitive decline in healthy older adults using fMRI. J. Alzheimers Dis 21, 871–885. [PubMed: 20634590]

Yang Z, Wen W, Jiang J, Crawford JD, Reppermund S, Levitan C, Sachdev PS, 2016 MRI markers of dementia in the eighth to eleventh decades of life. Alzheimers Dement. 12, P334–P335.

Yanker BA, 1996 Mechanisms of neuronal degeneration in Alzheimer's disease. Neuron 16, 921–932. [PubMed: 8630250]

Yu L, Boyle P, Schneider JA, Segawa E, Wilson RS, Leurgans S, Bennett DA, 2013 APOE ε4, Alzheimer's disease pathology, cerebrovascular disease, and cognitive change over the years prior to death. Psychol. Aging 28, 1015–1023. [PubMed: 23647000]

Zald DH, Pardo JV, 2000 Functional neuroimaging of the olfactory system in humans. Int. J. Psychophysiol 36, 165–181. [PubMed: 10742571]

Zhu Z, Johnson NF, Kim C, Gold BT, 2015 Reduced frontal cortex efficiency is associated with lower white matter integrity in aging. Cereb. Cortex 25, 138–146. [PubMed: 23960206]

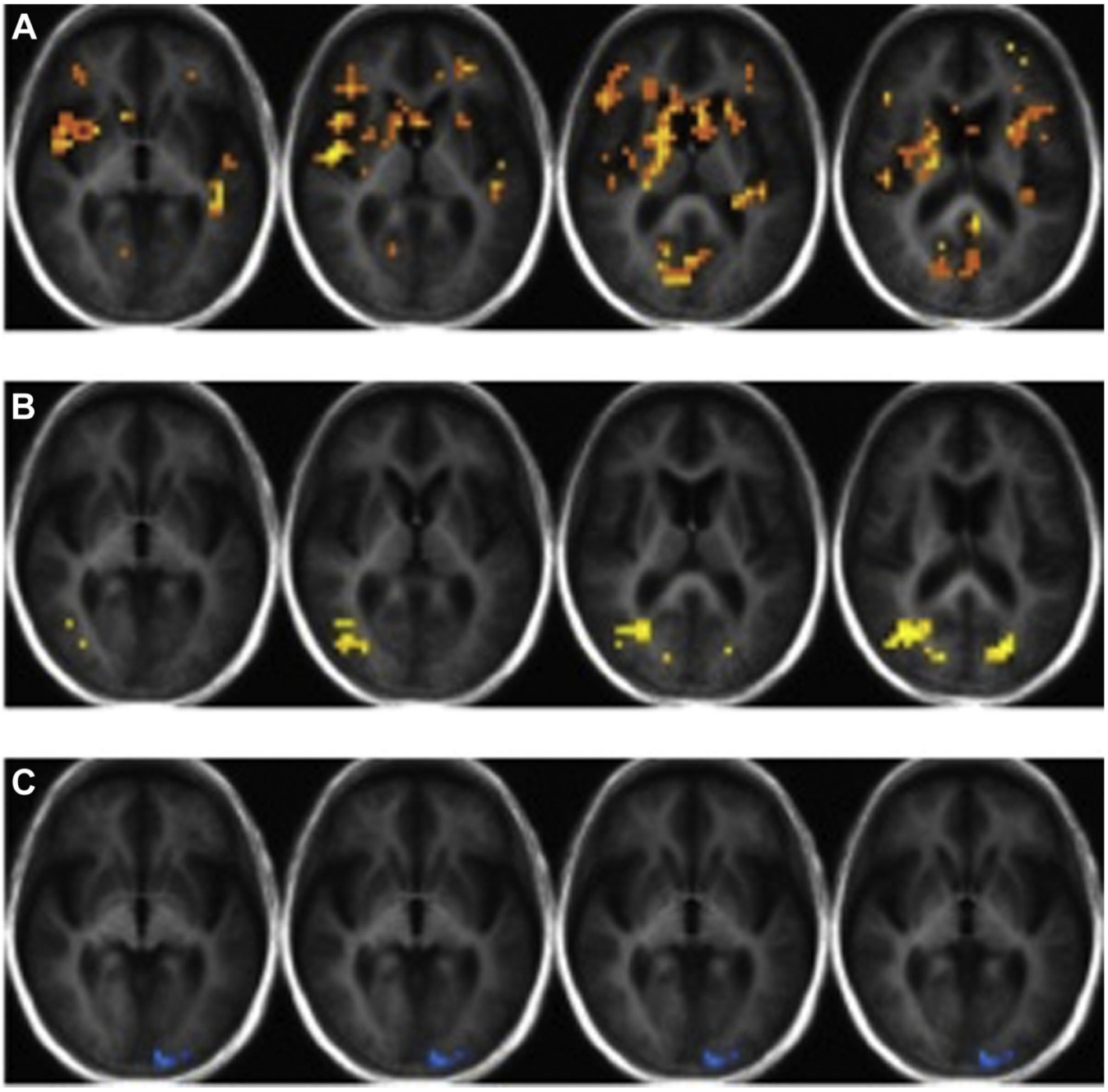

Fig. 1.

(A) Whole-brain activation during hits when functional activation of ε_4 carrier females was subtracted from ε_4 carrier males. Orange indicates the areas where ε_4 carrier males had greater activation compared to ε_4 carrier females. (B) Whole-brain activation during false positives when functional activation of ε_4 non-carriers was subtracted from ε_4 carriers. Yellow indicates the areas where ε_4 carriers had greater activation than ε_4 non-carriers. (C) Whole-brain activation during false positives when functional activation of ε_4 carrier females was subtracted from ε_4 carrier males. Blue indicates the areas where ε_4 carrier females had greater functional activation than ε_4 carrier males.

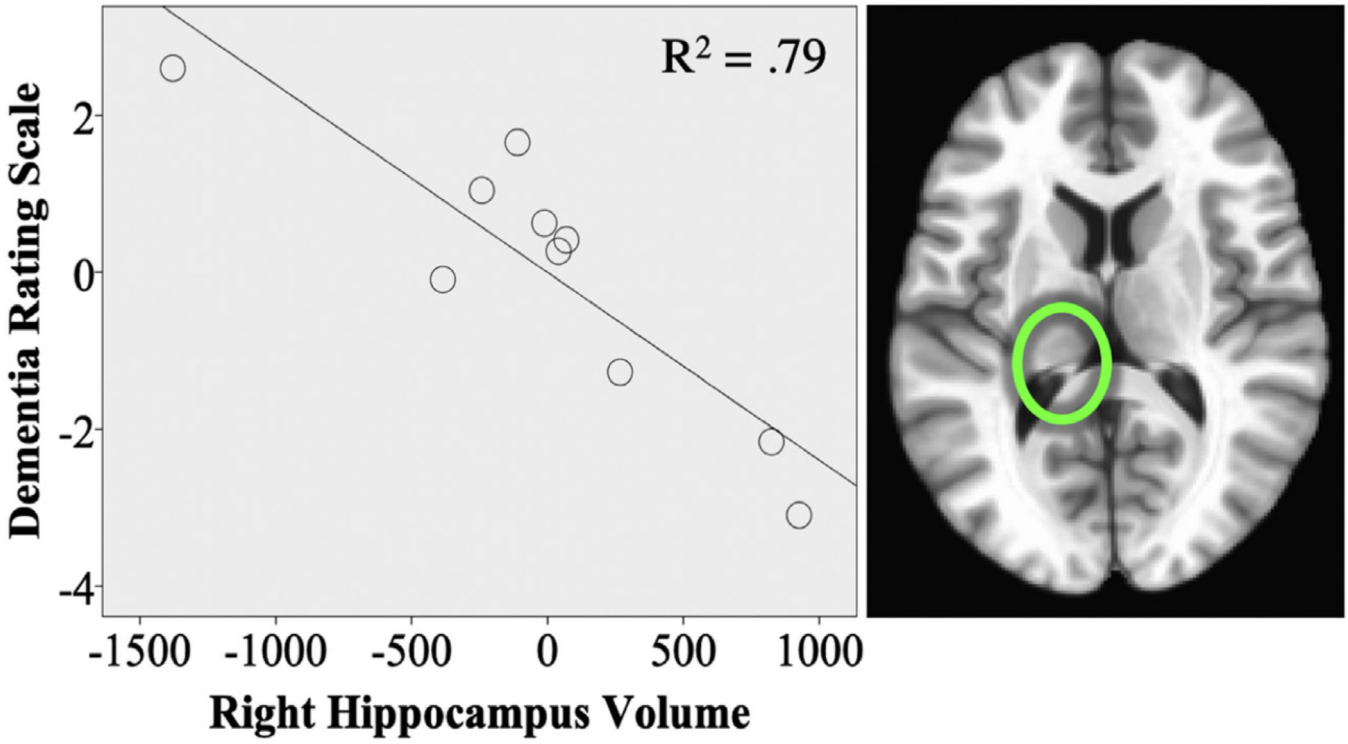

Fig. 2.

Association between right hippocampal volume (mm^3) and Dementia Rating Scale scores in male ε_4 non-carriers. Age and ICV were included as covariates. Abbreviation: ICV, intracranial volume.

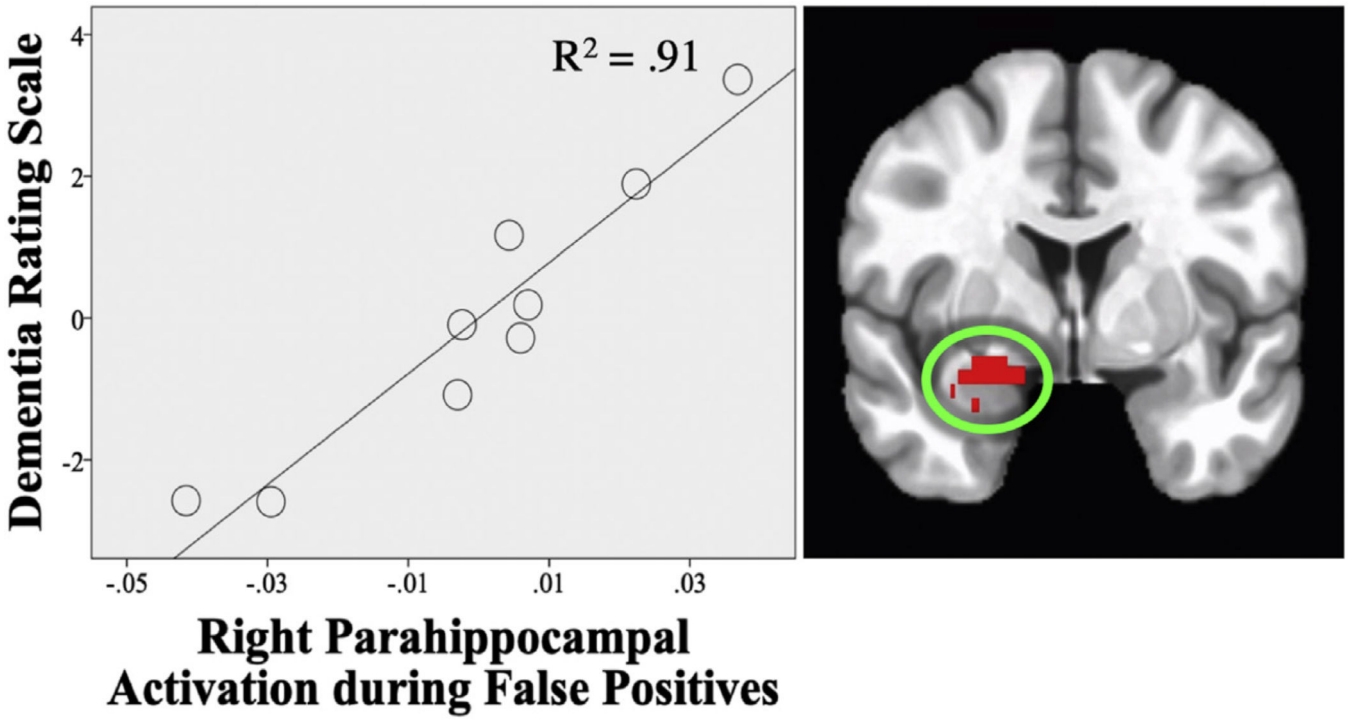

Fig. 3.

Partial regression plots using age, ICV, and structure volume as covariates. Association between Dementia Rating Scale scores and functional activation in the right parahippocampal gyrus during false positives in male ε_4 carriers. Abbreviation: ICV, intracranial volume.

Table 1

Participant demographics

Demographics	Mean (SD)				*F*			Significance
	ε_4 non-carriers		ε_4 carriers					
	Males (n = 10)	Females (n = 11)	Males (n = 9)	Females (n = 9)	ε_4 status	Sex	ε_4 × sex	
Age (y)	69.6 (3.7)	75 (7.1)	73 (7.7)	72.4 (8.9)	0.04	1.14	1.72	$p > 0.05$
Education (y)	15.5 (2.3)	15.3 (3.5)	15.8 (3.4)	15.3 (3.5)	0.02	0.09	0.03	$p > 0.05$
Odor threshold	5.5 (1.8)	5.0 (1.4)	4.4 (1.7)	5.8 (1.6)	0.05	0.85	3.10	$p > 0.05$
Odor ID	4.7 (1.3)	5.8 (1.4)	5.0 (1.5)	5.0 (1.8)	0.29	1.36	0.25	$p > 0.05$
DRS	140.6 (2.0)	138.0 (4.1)	139.4 (3.5)	138.8 (5.0)	0.02	1.78	0.44	$p > 0.05$

Key: DRS, Dementia Rating Scale; SD, standard deviation.

Table 2

Olfactory memory task performance rates

Memory measure	Mean (SD)				*F* (significance)		
	ε_4 non-carriers		ε_4 carriers				
	Males (n = 10)	Females (n = 11)	Males (n = 9)	Females (n = 9)	ε_4 status	Sex	ε_4 × sex
Hit rates							
Run 1	0.42 (0.13)	0.57 (0.11)	0.59 (0.12)	0.64 (0.17)	7.597[a] ($p = 0.01$)	4.829[a] ($p = 0.04$)	1.390 ($p > 0.05$)
Run 2	0.44 (0.17)	0.55 (0.14)	0.53 (0.21)	0.60 (0.15)	2.025 ($p > 0.05$)	2.234 ($p > 0.05$)	0.135 ($p > 0.05$)
FP rates							
Run 1	0.32 (0.15)	0.30 (0.11)	0.36 (0.12)	0.29 (0.09)	0.189 ($p > 0.05$)	1.27 ($p > 0.05$)	0.384 ($p > 0.05$)
Run 2	0.29 (0.15)	0.30 (0.14)	0.30 (0.16)	0.30 (0.11)	0.018 ($p > 0.05$)	0.012 ($p > 0.05$)	0.002 ($p > 0.05$)

Covariates appearing in the model are evaluated at the following values: age = 72.56.

Key: FP, false positives; SD, standard deviation.

[a]Denotes significance.

Table 3

Hippocampal volume (mm^3) and entorhinal cortex thickness (mm)

Structural measurements	Mean (SD)				*F* (significance)		
	ε_4 non-carriers		ε_4 carriers				
	Males (n = 10)	Females (n = 11)	Males (n = 9)	Females (n = 9)	ε_4 status	Sex	ε_4 × sex
Left hippocampus (mm^3)	2897.30 (869.75)	2957.45 (396.96)	2742.11 (656.94)	3400.44 (519.24)	0.16 ($p > 0.05$)	5.76[a] ($p = 0.02$)	0.949 ($p > 0.05$)
Right hippocampus (mm^3)	2923.40 (649.00)	3240.64 (538.18)	2994.78 (569.51)	3507.33 (462.88)	1.263 ($p > 0.05$)	8.59[a] ($p = 0.006$)	0.008 ($p > 0.05$)
Left ERC (mm)	2.45 (0.55)	2.64 (0.62)	2.22 (0.94)	2.61 (0.39)	0.532 ($p > 0.05$)	3.24 ($p > 0.05$)	0.003 ($p > 0.05$)
Right ERC (mm)	2.83 (0.49)	2.61 (0.18)	2.497 (0.39)	2.91 (0.39)	0.002 ($p > 0.05$)	0.66 ($p > 0.05$)	5.934[a] ($p = 0.02$)

Covariates appearing in the model are evaluated at the following values: age = 72.56, intracranial volume = 1,343,211.69.

Key: ERC, entorhinal cortex; SD, standard deviation.

[a]Denotes significance.

Table 4

Post hoc structural measurements

Structural measurements	Mean (SD)				F (significance)		
	ε_4 non-carriers		ε_4 carriers				
	Males (n = 10)	Females (n = 11)	Males (n = 9)	Females (n = 9)	ε_4 status	Sex	ε_4 × sex
Left caudate (mm^3)	3493.60 (439.56)	3531.55 (620.92)	4170.78 (666.75)	3616.56 (486.29)	3.47 ($p > 0.05$)	2.02 ($p > 0.05$)	2.10 ($p > 0.05$)
Right caudate (mm^3)	3492.30 (415.74)	3628.82 (960.68)	4219.78 (387.79)	3704.22 (541.19)	1.91 ($p > 0.05$)	0.58 ($p > 0.05$)	2.05 ($p > 0.05$)
Left putamen (mm^3)	4679.30 (824.49)	4658.55 (607.08)	5502.22 (741.86)	4930.44 (620.86)	5.52[a] ($p = 0.03$)	0.96 ($p > 0.05$)	2.61 ($p > 0.05$)
Right putamen (mm^3)	4424.10 (670.16)	4401.27 (668.75)	5419.67 (625.01)	4889.22 (628.16)	11.96[a] ($p = 0.002$)	1.22 ($p > 0.05$)	2.27 ($p > 0.05$)
Left parahippocampal gyrus (mm)	2.39 (0.34)	2.52 (0.35)	2.01 (0.38)	2.62 (0.44)	1.54 ($p > 0.05$)	9.65[a] ($p = 0.004$)	2.95 ($p > 0.05$)
Right parahippocampal gyrus (mm)	2.32 (0.24)	2.40 (0.36)	2.36 (0.38)	2.44 (0.16)	0.36 ($p > 0.05$)	0.77 ($p > 0.05$)	0.04 ($p > 0.05$)
Left isthmus cingulate gyrus (mm)	2.67 (0.21)	2.51 (0.23)	2.36 (0.15)	2.47 (0.17)	3.10[a] ($p = 0.09$)	0.57 ($p > 0.05$)	4.54[a] ($p = 0.041$)
Right isthmus cingulate gyrus (mm)	2.68 (0.24)	2.47 (0.35)	2.46 (0.24)	2.46 (0.19)	1.12 ($p > 0.05$)	0.90 ($p > 0.05$)	0.78 ($p > 0.05$)

MANCOVA controlled for age and ICV.

Key: ICV, intracranial volume; SD, standard deviation.

[a]Denotes significance.